ICSV13 - Vienna
The Thirteenth International Congress on Sound and Vibration
Vienna, Austria, July 2-6, 2006

STIFFNESS REQUIREMENTS FOR SLAB TRACK RAILWAYS: SOIL IMPROVEMENT VERSUS SLAB REINFORCEMENT, AND EFFECTS ON THE DYNAMIC RESPONSE

Michaël J.M.M. Steenbergen*[1], Andrei V. Metrikine[2] and Coenraad Esveld[1]

[1]Railway Engineering, Faculty of Civil Engineering and Geosciences, Delft University of Technology, Stevinweg 1, NL 2628 CN Delft, the Netherlands
[2]Structural Mechanics, Faculty of Civil Engineering and Geosciences, Delft University of Technology, Stevinweg 1, NL 2628 CN Delft, the Netherlands
M.J.M.M.Steenbergen@tudelft.nl

Abstract

The development of the ballast-less slab track, with applications especially on soft soil in combination with loading by high-speed trains, puts several specific engineering demands. One of these is how to provide the required stiffness of the track. Several approaches are possible: a first and most common approach is to apply massive soil improvements; a second approach is to increase the bending stiffness of the slab, as can be achieved by application of eccentric reinforcement. Both solutions have consequences for the dynamic track response. In this contribution, the model of a beam on elastic half-space subject to a moving load is employed to assess the effectiveness of these solutions from a dynamic viewpoint.

INTRODUCTION

The relatively new ballast-less slab track is applied worldwide on an increasing scale for high-speed lines. This is due to the fact that slab track has several advantages relative to ballasted track, such as a higher stability, the impossibility of rail buckling, less sensitivity to differential settlements, lower maintenance (reduction with 70-90% relative to ballasted track [2]), higher availability with the possibility of longer possession times, the prevention of churning up of ballast particles at high speed, and an increase of passenger comfort as well as safety, due to the higher track stability and the better alignment. Disadvantages are the high initial investment costs and a lower vibration and noise absorption.

The current design of slab track railways is based on the principle of a relatively flexible continuous or segmented concrete slab on top of a stiff substructure. Many high-speed lines are built in flat delta areas with relatively weak subgrades (Germany, Japan, Korea, Netherlands, Sweden). Therefore often massive cost-intensive soil improvements are necessary, especially to increase the critical train velocity.

According to the German school, based on highway design, the supporting layer (about 0.3 m), should have a substantial bearing stiffness. In many cases, soil improvement is necessary to meet the target value for the Young's modulus. Given this stiffness, also non-coherent block structures may be used, and differential settlements are excluded. The applied track designs have reinforcement in the neutral axis in order to control the crack width in the monolithic slab (Figure 1).

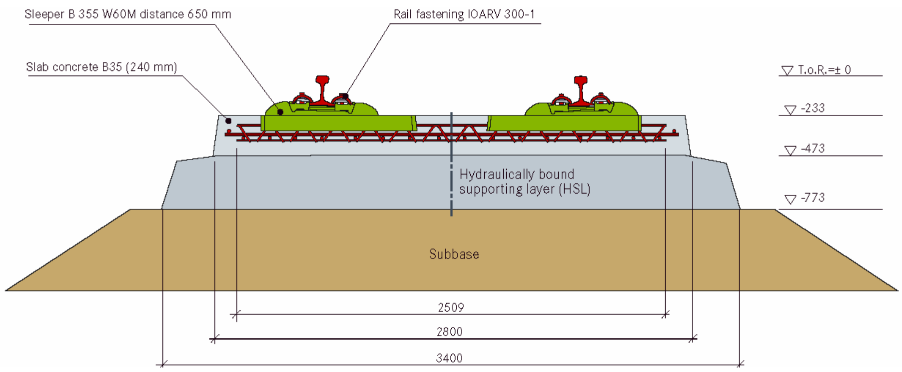

Figure 1 – Example of a slab track design, reinforced in the neutral axis (Rheda 2000)

These design principles do not account for the fact that a railway track, with a width approximately equal to the train width, is essentially different from a road pavement, where the width generally exceeds the vehicle width significantly. Railway tracks may be considered as predominantly 1D structures, whereas road superstructures should be considered as 2D plates when their structure is coherent. Furthermore, loading of a railway track is in general axially symmetric, allowing to disregard the variation in lateral moment. On the basis of the above, traditional slab track design may be stated to be rather conservative, and, due to the generally massive soil improvements, expensive relative to traditional ballasted concepts.

A more economic possibility to meet stiffness requirements is to increase the bending stiffness of the concrete slab track itself, e.g. applying an eccentric reinforcement. In literature [6], a comparative analysis of both methods has been performed from a static point of view. This contribution considers the question from a dynamic viewpoint.

MODEL FOR A SLAB TRACK, PROBLEM STATEMENT AND SOLUTION

The model which will be used to investigate the dynamic response of a slab track railway system to a running train axle is shown in Figure 2, along with some notations.

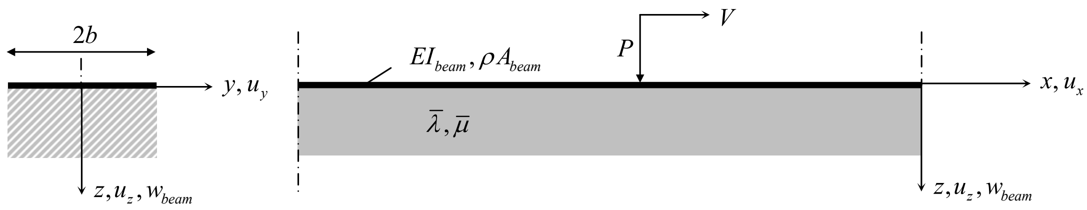

Figure 2 – Model for a slab track: vertical planes across and along the track axis

According to recent investigations on slab-track by Savidis and Bergmann [4], realistic results can be obtained with the help of the adopted basic model of a beam on visco-elastic half-space, subject to a moving load. The beam cross-section is considered as infinitely rigid, and the problem is assumed to be length-invariant.

The total dynamic stiffness of the track under a moving train axle depends on both the dynamic stiffness of the slab and that of the half-space against the slab; the latter will be derived first. Disregarding the travelling load, the dynamic interaction of the beam and the half-space is governed by the following equations:

- Equation of motion for an inner element of the half-space (Lamé equation):

$$\bar{\mu}\nabla^2 \boldsymbol{u} + (\bar{\lambda} + \bar{\mu})\nabla(\nabla \cdot \boldsymbol{u}) = \rho \boldsymbol{u}_{,tt} \tag{1}$$

where $\boldsymbol{u}$ denotes the displacement vector, $\bar{\lambda} = \lambda + \lambda'\partial/\partial t$, $\bar{\mu} = \mu + \mu'\partial/\partial t$ are differential operators with Lamé constants λ and μ and ρ denotes the mass density of the half-space material (modelled according to Voight's model).

- Interface conditions between the beam and the half-space:

$$\begin{aligned} &\int_{-b}^{b} \sigma_{zz}(x,y,0,t)dy = EI_{beam} w_{beam}(x,t)_{,xxxx} + \rho A_{beam} w_{beam}(x,t)_{,tt} && |y| < b \\ &\boldsymbol{u}(x,y,0,t) = \begin{bmatrix} 0 & 0 & w_{beam}(x,t) \end{bmatrix}^T && |y| < b \end{aligned} \tag{2}$$

- Boundary conditions at the free part of the surface:

$$\boldsymbol{\sigma}(x,y,0,t) = \begin{bmatrix} 0 & 0 & 0 \end{bmatrix}^T \qquad |y| > b \text{ where } \boldsymbol{\sigma} = \begin{bmatrix} \sigma_{zx} & \sigma_{zy} & \sigma_{zz} \end{bmatrix}^T \tag{3}$$

To derive the dynamic stiffness of the half-space against the beam, a contact force $\boldsymbol{F}(x,t)$ between the beam and the half-space is introduced ($\boldsymbol{F}$ has the dimension of force per unit of length). In a following step, the interface conditions (2) are discretised, which will allow for a replacement of the integral of the normal tractions in (2) by a finite sum, as shown in Figure 3.

Across the interface, the continuous variable y is changed into a discrete variable y_n, positioned at the middle of an interval n with width Δy. Within each subdomain n, stresses are assumed invariant and displacement compatibility is required along the lines $y = y_n$; $y_n = -b + \Delta y \cdot (2n-1)/2$ where $1 \le n \le N$ with $N = 2b/\Delta y$.

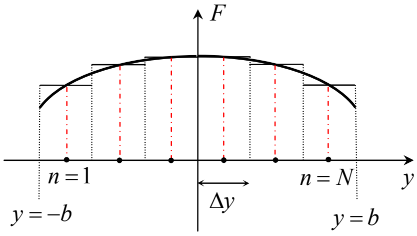

Figure 3 – Discretisation of the stress field across the slab-soil interface

Eqs. (2) are now rewritten in terms of running coordinate y_m:

$$\boldsymbol{u}(x, y_m, 0, t) = \begin{bmatrix} 0 & 0 & w_{beam}(x,t) \end{bmatrix}^T \qquad 1 \le m \le N \tag{4}$$

$$\boldsymbol{\sigma}(x, y, 0, t) = \sum_{n=1}^{N} \frac{\boldsymbol{F}_n(x,t)}{\Delta y} H\left(\frac{\Delta y}{2} - |y - y_n|\right) \qquad |y| < b\text{; } \boldsymbol{F} = \begin{bmatrix} F_x & F_y & F_z \end{bmatrix} \tag{5}$$

The solution to the equation of motion (1) is commonly found applying the Helmholtz decomposition of the displacement vector field into a scalar potential and a vector potential with three elements, yielding the decoupled compressional and shear wave equations. Since the steady-state behaviour is considered, these equations can be solved applying Fourier integral transforms with respect to the spatial coordinates *x*, *y* and time *t*, leading to a set of ordinary differential equations with 4 general exponential solutions for the 4 Fourier-transformed potentials. The 4 unknown constants in these solutions can be found applying the boundary conditions.

The stress boundary conditions (5) can be transformed to the k_x, k_y, ω-domain. This is not true for the displacement boundary conditions (4), where *y*-transformation is not possible. The final solution should therefore be found in the k_x, y, ω-domain. As a result of this procedure (described in [5]), the following integral equation is obtained:

$$\sum_{l=m-1}^{m-N} \boldsymbol{I}^{(l)} \tilde{\tilde{\boldsymbol{F}}}^{(n)} = \begin{bmatrix} 0 & 0 & 2\pi\tilde{\mu}\Delta y \tilde{\tilde{w}}_{beam} \end{bmatrix}^T \qquad 1 \le m \le N \tag{6}$$

The elements of the matrices $\boldsymbol{I}^{(l)}$ are given by ($1 - N \le l \le N - 1$):

$$I_{11}^{(l)} = -i\frac{1}{k_x}\int_{-\infty}^{\infty} \frac{1}{\xi \bar{R}_s} \varepsilon d\xi - i\frac{1}{k_x}\int_{-\infty}^{\infty} \frac{4\left(1+\xi^2\right) - 3\beta_s^2 - 4\bar{R}_p\bar{R}_s}{\xi \bar{R}_s \bar{\Delta}} \varepsilon d\xi \tag{7}$$

$$I_{22}^{(l)} = -i\frac{1}{k_x}\int_{-\infty}^{\infty} \frac{1}{\xi \bar{R}_s} \varepsilon d\xi - i\frac{1}{k_x}\int_{-\infty}^{\infty} \xi \frac{4\left(1+\xi^2\right) - 3\beta_s^2 - 4\bar{R}_p\bar{R}_s}{\bar{R}_s \bar{\Delta}} \varepsilon d\xi \tag{8}$$

$$I_{12}^{(l)} = I_{21}^{(l)} = -i\frac{1}{k_x}\int_{-\infty}^{\infty} \frac{4\left(1+\xi^2\right) - 3\beta_s^2 - 4\bar{R}_p\bar{R}_s}{\bar{R}_s \bar{\Delta}} \varepsilon d\xi \tag{9}$$

$$I_{13}^{(l)} = -I_{31}^{(l)} = \frac{1}{k_x}\int_{-\infty}^{\infty} \frac{2\left(1+\xi^2\right)-\beta_s^2-2\bar{R}_p\bar{R}_s}{\xi\bar{\Delta}}\varepsilon\, d\xi \qquad (10)$$

$$I_{23}^{(l)} = -I_{32}^{(l)} = \frac{1}{k_x}\int_{-\infty}^{\infty} \frac{2\left(1+\xi^2\right)-\beta_s^2-2\bar{R}_p\bar{R}_s}{\bar{\Delta}}\varepsilon d\xi \qquad (11)$$

$$I_{33}^{(l)} = -i\beta_s^2\frac{1}{k_x}\int_{-\infty}^{\infty}\frac{\bar{R}_p}{\xi\bar{\Delta}}\varepsilon\, d\xi \quad \text{where } \varepsilon = \left(e^{ik_x\xi\Delta y\left(l-\frac{1}{2}\right)} - e^{ik_x\xi\Delta y\left(l+\frac{1}{2}\right)}\right) \qquad (12)$$

The following notations have been used:

$$\xi = k_y/k_x,\ v_{ph} = \omega/k_x,\ \beta_{p,s} = v_{ph}/\tilde{c}_{p,s}\ \ \tilde{c}_p^2 = c_p^2 - i\omega(\lambda'+2\mu')/\rho,\ \tilde{c}_s^2 = c_s^2 - i\omega\mu'/\rho,$$
$$c_P = \sqrt{(\lambda+2\mu)/\rho},\ c_S = \sqrt{\mu/\rho},\ \bar{R}_{p,s} = \sqrt{1+\xi^2-\beta_{p,s}^2},$$
$$\bar{\Delta} = 4\bar{R}_p\bar{R}_s\left(1+\xi^2\right)-\left(2\left(1+\xi^2\right)-\beta_s^2\right)^2 \qquad (13)$$

The integrals (7-12) can be evaluated numerically; due to the material damping in the half-space the integrands do not have singularities on the integration path. When integrating, the well-known 4 regimes of the phase speed of longitudinal waves can be distinguished: the sub-Rayleigh regime, the subsonic regime, the trans-sonic regime and the supersonic regime.

THE TOTAL GENERALISED DYNAMIC TRACK STIFFNESS AND ITS DYNAMIC RESPONSE

In accordance with the concept introduced by Dieterman and Metrikine [1], the dynamic stiffness vector for an arbitrary strip n and the total equivalent dynamic stiffness of the half-space under the beam are introduced as, respectively:

$$\boldsymbol{\chi}^{(n)}(k_x, y_n, \omega) = -\frac{\tilde{\tilde{\boldsymbol{F}}}^{(n)}}{\tilde{\tilde{w}}_{beam}};\quad \boldsymbol{\chi} = -\frac{1}{\tilde{\tilde{w}}_{beam}}\sum_{n=1}^{N}\tilde{\tilde{\boldsymbol{F}}}^{(n)} \qquad (14)$$

This stiffness allows for a reformulation of the problem of the beam on half-space to a beam on a 1-D elastic foundation, with complex stiffness χ depending on the frequency and wavenumber of flexural waves in the beam. Eq. (6), in terms of this stiffness, reads:

$$\sum_{l=m-1}^{m-N}\boldsymbol{I}^{(l)}\boldsymbol{\chi}^{(m-l)} = \begin{bmatrix}0 & 0 & -2\pi\mu\Delta y\end{bmatrix}^T \qquad 1\le m\le N \qquad (15)$$

From this matrix equation, the vertical equivalent dynamic soil stiffness against the slab can be solved. For the determination of the total vertical stiffness of the track to a frequency component of the loading spectrum by a moving train axle, the beam equation must be introduced. Adopting a complex form of the load with frequency ω_0, the first interface condition from (2) enhances to:

$$EI_{beam}w_{beam}(x,t)_{,xxxx} + \rho A_{beam}w_{beam}(x,t)_{,tt} - \int_{-b}^{b}\sigma_{zz}(x,y,0,t)dy = -Pe^{i\omega_0 t}\delta(x-Vt) \quad (16)$$

The solution of in the frequency-wavenumber domain is given by:

$$\tilde{\tilde{w}}_{beam}(k_x,\omega) = -2\pi P\frac{\delta(\omega_0+\omega-Vk_x)}{D_{beam}(k_x,\omega)+\chi_z(k_x,\omega)}; \quad D_{beam} = EI_{beam}k_x^4 - \rho A_{beam}\omega^2 \quad (17)$$

In general, the beam can be considered as loaded by different types of loading in the space-time domain, in vertical direction. Each loading on the beam may be transformed to the wavenumber-frequency domain. The stiffness of the beam – half-space system under this generalised loading is a function of both frequency and wavenumber. This stiffness appears in the denominator of (17) as a summation of the vertical dynamic stiffness of the half-space under the beam and that of the free beam. It will be referred to as a 'generalised dynamic stiffness', designated as K_z, and used as a parameter to characterize the 'overall stiffness' of the track.

$$\mathrm{K}_z(k_x,\omega) = D_{beam} + \chi_z = EI_{beam}k_x^4 - \rho A_{beam}\omega^2 + \chi_z(k_x,\omega) \quad (18)$$

An increase of the slab stiffness can be represented by an increase in EI, whereas a soil improvement leads to a change of χ_z. An increase of the beam flexural stiffness is proportional to k_x^4, which means that the stiffness increase is much more efficient for high wavenumbers or short waves than for long waves. The change of K_z due to an increase of the soil Young's modulus depends on the change in equivalent soil stiffness, the actual magnitude of which depends on both ω and k_x.

To enable numerical simulations, representative parameter values are chosen: slab parameters: $2b = 3.20\,\mathrm{m}$, $A = 1.10\,\mathrm{m}^2$, $I = 0.011\,\mathrm{m}^4$, $\rho = 2400\,\mathrm{kgm}^{-3}$, $E = 20\cdot 10^9\,\mathrm{Nm}^{-2}$, or: $EI = 2.20\cdot 10^8\,\mathrm{Nm}^2$ and $\rho A = 2640\,\mathrm{kgm}^{-1}$; half-space (soil) parameters: $E_{soil} = 8\cdot 10^7\,\mathrm{Nm}^{-2}$, $\upsilon = 0.3$, $\rho = 1960\,\mathrm{kgm}^{-3}$. A negligible damping is adopted, leading to quasi-undamped solutions.

In Figure 4, K_z is depicted as a function of v_{ph}, for $E_{soil} \to 2E_{soil}$ and $EI_{beam} \to 2EI_{beam}$ respectively. A short wavelength (4.2 m) relative to the slab width (3.2 m) is considered as well as a long one (62.8 m). The contribution of the dynamic soil stiffness to the total stiffness is shown (green line) in both graphs: it is clear that for short waves and high frequencies this contribution is significantly higher than for long waves and low frequencies. Limiting considerations – for practice – to the subcritical (sub-Rayleigh) train speed regime, it may be concluded from Figure 4 that for long waves (or low frequencies) soil improvement is a better solution, whereas for short waves (or high frequencies) the contribution of the increase of the slab stiffness may easily exceed that of an increase in the soil stiffness.

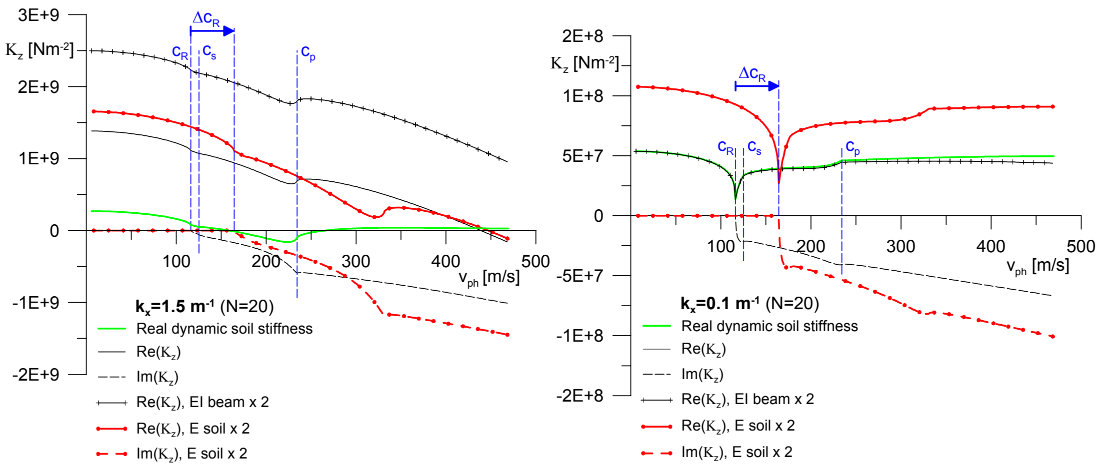

Figure 4 – Effects of a doubling of the beam flexural stiffness and the soil Young's modulus on the generalized dynamic track stiffness for short waves (left) and long waves (right).

It can be shown that disregarding the slab mass, K_z for short waves is almost uniformly distributed over v_{ph} (or ω). For given k_x, the track mass reduces K_z proportional to the 2nd power of v_{ph}. Therefore, for high phase velocities and short waves/high frequencies the slab mass reduces the dynamic track stiffness drastically.

It should be remarked that the modulus of the total half-space has been increased, whereas in reality a soil improvement is limited to the vicinity of the track. However, for a constant load moving at subcritical velocity over a half-space, the eigenfield of the load is localized in its vicinity; no wave radiation occurs [3]. For harmonic loading on inhomogeneous soil, the error increases with the intensity of radiation, or, with frequency. Therefore, the model is applicable only for subcritical loading cases where the non-oscillating part of the loading prevails.

The displacement amplitude of the slab track under the travelling harmonic load is given by the absolute value of the inverse transform of (17) for $x = Vt$:

$$\left|w_{beam}(Vt,t)\right| = \frac{P}{2\pi}\left|\int_{-\infty}^{\infty} \frac{1}{D_{beam}\left(k_x, k_x V - \omega_0\right) + \chi_z\left(k_x, k_x V - \omega_0\right)} dk_x\right| \tag{19}$$

In Figure 5 this amplitude is shown as a function of ω_0 (1.6-80 Hz) for a reference track, a track on an improved soil with doubled Young's modulus, and a slab with doubled *EI*; $P = 225\,\text{kN}$ and $V = 40\,\text{m/s}$ (144 km/h). It can be shown that, in the subcritical regime, the velocity influence on the track frequency response is negligible. It is observed that the frequency response function (FRF) for the improved soil shows a lower vibration level for low frequencies, whereas the performance for higher frequencies is worse. The FRF for an increase of the slab bending stiffness shows a lower track vibration level for the whole frequency domain. Further, for low frequencies the soil improvement is most effective, whereas in the high-frequency range the slab stiffening is much more effective, as was concluded before. Therefore, the whole load spectrum should be accounted for in intelligent slab track design.

In Figure 5, three important frequencies for the dynamic track response are indicated: the sleeper passing frequency $\omega_{sl} = 2\pi V / d_{sl}$ ($d_{sl} = 0.6$ m), the axle passing frequency $\omega_{axle} = 2\pi V / d_{axle}$ ($d_{axle} = 3$ m) and the bogie passing frequency $\omega_{bogie} = 2\pi V / d_{bogie}$ ($d_{bogie} = 18.7$ m). Figure 5 shows that to reduce the response at ω_{bogie}, generally soil improvement is better. A general conclusion on ω_{axle} cannot be drawn, whereas for reduction at ω_{sl} an increase of the slab stiffness is most effective.

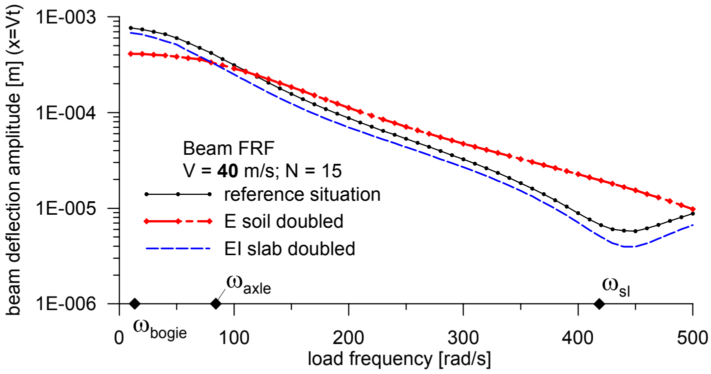

Figure 5 – Effects of an increase of the slab stiffness and a soil improvement on the slab FRF

CONCLUSIONS

Soil improvement and increasing the slab bending stiffness have been considered as possibilities to meet stiffness requirements for slab track high-speed railways. The generalised vertical dynamic track stiffness against an arbitrary loading in the frequency-wavenumber domain has been introduced and compared for both methods. For short waves relative to the beam width and high frequencies an increase of the track stiffness proofs most effective, whereas for much longer waves and low frequencies soil improvement is a better solution. The latter also has the advantage of increasing the critical train velocity. An optimum design of high speed slab track railways on soft soil accounts for the expected loading spectrum.

REFERENCES

[1] H.A. Dieterman, A.V. Metrikine, "The equivalent stiffness of a half-space interacting with a beam. Critical velocities of a load moving along the beam", Eur. J. Mech. A/Solids, **15**, 67-90 (1996).

[2] C. Esveld, *Modern Railway Track*. (MRT-Productions, Zaltbommel, 2001)

[3] D.L. Lansing, "The displacements in an elastic half-space due to a moving concentrated normal load", NASA TR R-238 (1966).

[4] S.A. Savidis, S. Bergmann, "Slab track vibration and stress distribution induced by train passage", Eurodyn 2005, C. Soize, G.I. Schuëller (Eds), Millpress, Rotterdam, 651-656 (2005).

[5] M.J.M.M. Steenbergen, A.V. Metrikine, "The effect of the interface conditions on the dynamic response of a beam on a half-space to a moving load", Eur. J. Mech. A/Solids, acc. for publ. (2006).

[6] J.M. Zwarthoed, V.L. Markine, C. Esveld, "Slab track design: flexural stiffness versus soil improvement", Rail-Tech Europe 2001, Utrecht, 1-22 (2001).